A New Geometry for Homoleptic Organochromium Compounds

Pablo J. Alonso, Juan Forniés, M. Angeles García-Monforte, Antonio Martín, and Babil Menjón*

Instituto de Ciencia de Materiales de Aragón, Facultad de Ciencias, Universidad de Zaragoza-CSIC, C/ Pedro Cerbuna 12, E-50009 Zaragoza, Spain

Received February 3, 2004

$[NBu_4]_2[Cr(C_6F_5)_5]$ (**1**) has been obtained by low-temperature treatment of $[CrCl_3(THF)_3]$ with LiC_6F_5. The five-coordinate anion $[Cr(C_6F_5)_5]^{2-}$ has been found to be square pyramidal by X-ray diffraction methods. The *SPY*-5 geometry is unprecedented for homoleptic organochromium compounds. EPR data for this paramagnetic $S = 3/2$ system (d^3 electron configuration) point to the existence of two types of Cr^{III} centers with very similar coordination environments. A comparison with the titanium(III) isoleptic species $[Ti(C_6F_5)_5]^{2-}$ allows us to conclude that the fact that $[Cr(C_6F_5)_5]^{2-}$ in **1** adopts a *SPY*-5 structure must be due to electronic reasons associated with the electron configuration of the metal center.

Introduction

Organochromium derivatives have fascinated chemists for more than a century. Early attempts to prepare them revealed that the products obtained by treating different inorganic chromium substrates with Grignard reagents readily suffered hydrolytic[1] or reductive coupling reactions,[2] preventing their isolation. This failure along with many others contributed to creating the (now odd) idea that M−C bonds were thermodynamically unstable for transition metals. Until the second half of last century, this arid terrain was to produce only two successful sets of results: the methylplatinum complexes $[\{PtMe_3\}_4(\mu\text{-}X)_4]$[3] and Hein's *Chromphenylverbindungen*.[4] The former were unique but understandable compounds; the latter have gone down in the history of chemistry as a clear example of the difficulties encountered in rationalizing experimental facts without the proper theoretical frame. Once the real nature of these intriguing compounds, as low-valent (π-arene)Cr derivatives, was disclosed,[5] renewed efforts were devoted to the initial task of synthesizing authentic σ-organochromium compounds, which were indeed obtained in various oxidation states and stoichiometries. It soon became clear that coordinative saturation was an important factor determining the stability of σ-organochromium(III) compounds, and thus, a large number of them could be prepared by using suitable ancillary ligands.[6] However, homoleptic species $[CrR_n]^{q-}$ ($q = 0, \pm1, \pm2, ...$) in which a single ligand R is responsible for the stability of the compound are still rare. To the best of our knowledge, the only structurally characterized homoleptic σ-organochromium(III) species for the whole range of $n = 0-6$ stoichiometries are $[Cr\{CH(SiMe_3)_2\}_3]$,[7] $[Li(THF)_4][Cr(C_6Cl_5)_4]$,[8] $[\{Na(OR_2)_2\}_2\{CrPh_5\}]$,[9] $[\{Li(OEt_2)\}_3\{CrPh_6\}]$,[10] and $[\{Li_3(1,4\text{-dioxane})_3(CrMe_6)\}_\infty]$.[11] We now report on a new representative of this important type of compounds.

Experimental Section

General working techniques are as given elsewhere.[12] The starting materials $[CrCl_3(THF)_3]$[13] and LiC_6F_5[14] were prepared using previously reported methods.

CAUTION: Compound **1** has been found to explode by percussion, but sometimes for no obvious reason.

Synthesis of $[NBu_4]_2[Cr(C_6F_5)_5]$ (1). To a solution of LiC_6F_5 (ca. 20 mmol) in Et_2O (70 cm^3) at −78 °C was added $[CrCl_3(THF)_3]$ (1.16 g, 3.10 mmol). The suspension was allowed to warm to −30 °C, and after the addition of NBu_4Br (1.00 g, 3.10 mmol), the temperature was further allowed to rise to 0 °C. After 3 h of stirring at this temperature, a green oil had

* To whom correspondence should be addressed. E-mail: menjon@unizar.es.

(1) Sand, J.; Singer, F. *Liebigs Ann. Chem.* **1903**, *329*, 190.
(2) Bennett, G. M.; Turner, E. E. *J. Chem. Soc., Trans.* **1914**, *105*, 1057.
(3) Pope, W. J.; Peachey, S. J. *Proc. Chem. Soc., London* **1907**, *23*, 86. Pope, W. J.; Peachey, S. J. *J. Chem. Soc., Trans.* **1909**, *95*, 517.
(4) Hein, F. *Ber. Dtsch. Chem. Ges.* **1919**, *52*, 195. Hein, F. *Ber. Dtsch. Chem. Ges.* **1921**, *54*, 1905. For reviews on these and subsequent works, see: Uhlig, E. *Organometallics* **1993**, *12*, 4751. Seyferth, D. *Organometallics* **2002**, *21*, 2800. Seyferth, D. *Organometallics* **2002**, *21*, 1520.
(5) Fischer, E. O.; Seus, D. *Chem. Ber.* **1956**, *89*, 1809. Zeiss, H. H.; Tsutsui, M. *J. Am. Chem. Soc.* **1957**, *79*, 3062.
(6) Kirtley, S. W. In *Comprehensive Organometallic Chemistry*; Wilkinson, G., Stone, F. G. A., Abel, E. W., Eds.; Pergamon Press: Oxford, UK, 1982; Vol. 3, Section 26.1, pp 783−951. Winter, M. J.; Woodward, S. In *Comprehensive Organometallic Chemistry II*; Abel, E. W., Stone, F. G. A., Wilkinson, G., Eds.; Elsevier Science Ltd.: Oxford, UK, 1995; Vol. 5, Chapter 5, pp 281−329.
(7) Barker, G. K.; Lappert, M. F. *J. Organomet. Chem.* **1974**, *76*, C45. Barker, G. K.; Lappert, M. F.; Howard, J. A. K. *J. Chem. Soc., Dalton Trans.* **1978**, 734.
(8) (a) Alonso, P. J.; Falvello, L. R.; Forniés, J.; García-Monforte, M. A.; Martín, A.; Menjón, B.; Rodríguez, G. *Chem. Commun.* **1998**, 1721. (b) Alonso, P. J.; Forniés, J.; García-Monforte, M. A.; Martín, A.; Menjón, B.; Rillo, C. *Chem. Eur. J.* **2002**, *8*, 4056.
(9) (a) Hein, F.; Schmiedeknecht, K. *J. Organomet. Chem.* **1966**, *5*, 454. (b) Müller, E.; Krause, J.; Schmiedeknecht, K. *J. Organomet. Chem.* **1972**, *44*, 127 (in this work $4R_2O = 3Et_2O{\cdot}THF$).
(10) (a) Hein, F.; Weiss, R. *Z. Anorg. Allg. Chem.* **1958**, *295*, 145. (b) Olmstead, M. M.; Power, P. P.; Shoner, S. C. *Organometallics* **1988**, *7*, 1380.
(11) Kurras, E.; Otto, J. *J. Organomet. Chem.* **1965**, *4*, 114. Krausse, J.; Marx, G. *J. Organomet. Chem.* **1974**, *65*, 215.
(12) Ara, I.; Forniés, J.; García-Monforte, M. A.; Martín, A.; Menjón, B. *Chem. Eur. J.* **2004**, *10*, 4186.
(13) Boudjouk, P.; So, J. H.; Ackermann, M. N.; Hawley, S. E.; Turk, B. E. *Inorg. Synth.* **1992**, *29*, 108.
(14) Usón, R.; Laguna, A. *Inorg. Synth.* **1982**, *21*, 71.

10.1021/om0499106 CCC: $30.25
Publication on Web 02/11/2005

Table 1. Crystal Data and Structure Refinement for $1\cdot CH_2Cl_2$

empirical formula	$C_{63}H_{74}Cl_2CrF_{25}N_2$
fw	1457.14
cryst size (mm)	0.46 × 0.30 × 0.15
temperature (K)	100(2)
cryst syst	monoclinic
space group	$P2_1/n$
a (pm)	1187.42(6)
b (pm)	4399.4(2)
c (pm)	1255.91(6)
β (deg)	96.715(1)
V (nm^3)	6.5159(6)
Z	4
d_c (g cm^{-3})	1.485
μ (mm^{-1})	0.370
F(000)	2996
θ range (deg)	1.70−25.07
index range	$-14 \le h \le 14$ $-52 \le k \le 47$ $-14 \le l \le 11$
no. of reflns collected	35 741
no. of unique reflns	11 510, $R_{int} = 0.0389$
completeness to $\theta = 25.07°$	99.5%
transmission	max 0.9465 min 0.8481
no. of data/restrts/params	11 510/0/838
final R indices ($I > 2\sigma(I)$)[a]	$R_1 = 0.0388$, $wR_2 = 0.0603$
R indices (all data)	$R_1 = 0.0640$, $wR_2 = 0.0637$
GOF[b] on F^2	0.964

[a] $R_1 = \sum(|F_o| - |F_c|)/\sum|F_o|$; $wR_2 = [\sum w(F_o^2 - F_c^2)^2/\sum w(F_c^2)^2]^{1/2}$; $w = [\sigma^2(F_o^2) + (g_1P)^2 + g_2P]^{-1}$; $P = (1/3)[\max\{F_o^2,0\} + 2F_c^2]$. [b] Goodness-of-fit = $[\sum w(F_o^2 - F_c^2)^2/(n_{obs} - n_{param})]^{1/2}$.

formed. It was decanted, washed with Et_2O (3 × 5 cm^3), and extracted in CH_2Cl_2 (70 cm^3) at 0 °C. The solvent in the extract was concentrated to a final volume of ca. 20 cm^3, and the slow diffusion of a Et_2O layer (60 cm^3) into it at −30 °C yielded **1** as a microcrystalline light green solid (2.09 g; 49% yield based on the chromium precursor). Anal. Found: C 53.6, H 5.2, N 2.0. $C_{62}H_{72}CrF_{25}N_2$ requires: C 54.3, H 5.3, N 2.0. IR (KBr): $\tilde{\nu}_{max}$/cm^{-1} = 1629 (m), 1531 (m), 1495 (vs), 1436 (vs), 1369 (m), 1324 (m), 1273 (w), 1237 (m), 1058 (s), 1041 (vs), 947 (vs; C_6F_5: C−F),[15] 882 (w; NBu_4^+), 800 (w; C_6F_5: X-sensitive vibr.),[15] 755 (sh) 742 (w), 713 (w), 600 (w) and 479 (w).

Crystals suitable for X-ray diffraction analysis with formula $[NBu_4]_2[Cr(C_6F_5)_5]\cdot CH_2Cl_2$ were obtained by slow diffusion of a layer of Et_2O (30 cm^3) into a solution of 50 mg of **1** in 10 cm^3 of CH_2Cl_2 at −30 °C.

Crystal Data for $1\cdot CH_2Cl_2$. Crystal data and other details of the structure analysis are presented in Table 1. A single crystal was mounted on a quartz fiber in a random orientation and held in place with a fluorinated oil. Data collection was performed on a Bruker Smart CCD area detector diffractometer using graphite-monocromated Mo Kα radiation (λ = 71.073 pm) with a nominal crystal to detector distance of 6.0 cm. Unit cell dimensions were initially determined from the positions of 277 reflections in 90 intensity frames measured at 0.3° intervals in ω and subsequently refined on the basis of positions of 6607 reflections from the main data set. A hemisphere of data was collected based on three ω-scans runs (starting $\omega = -28°$) at values $\phi = 0°$, 90°, and 180° with the detector at $2\theta = 28°$. At each of these runs, frames (606, 435, and 230, respectively) were collected at 0.3° intervals and 10 s per frame. The diffraction frames were integrated using the SAINT package[16] and corrected with SADABS.[17] Lorentz and polarization corrections were also applied. The structure was solved by direct methods and refined against F^2 using the SHELXL-97 program,[18] converging to final residual indices given in Table 1. All non-hydrogen atoms were assigned anisotropic displacement parameters and refined without positional constraints. All hydrogen atoms were constrained to idealized geometries and assigned isotropic displacement parameters 1.2 times the U_{iso} value of their attached carbon atoms (1.5 times for methyl hydrogen atoms). CCDC reference number 256011.

EPR Measurements. X- and Q-band EPR spectra were registered in a Bruker ESP380 spectrometer. The magnetic field was measured with a Bruker ER035M gaussmeter. A Hewlett-Packard HP5350B frequency counter was used to determine the microwave frequency. W-band measurements were performed at the EPR laboratory of the ETH (Zürich, Switzerland) using a Bruker ElexSys E680 spectrometer. Measurements at 77.3 K were performed using an immersion quartz dewar.

Results and Discussion

Synthesis and Structural Characterization. The reaction of $[CrCl_3(THF)_3]$ with LiC_6F_5 in Et_2O at −78 °C, followed by addition of NBu_4Br at −30 °C, gave—after the appropriate workup—$[NBu_4]_2[Cr(C_6F_5)_5]$ (**1**) as a light green solid in reasonable yield (eq 1). Microcrystalline samples of **1** are not only air-sensitive and thermally labile but also explosive by percussion, and hence much caution must be taken in its handling.

$$[CrCl_3(THF)_3] + LiC_6F_5 \xrightarrow{+\,NBu_4Br} \underset{\mathbf{1}}{[NBu_4]_2[Cr(C_6F_5)_5]} \quad (1)$$

In the IR spectrum of **1**, the most significant feature is the absorption assignable to the X-sensitive vibration mode of the C_6F_5 group,[15] which appears as a weak band at 800 cm^{-1}. The cyclic voltammogram of **1** in CH_2Cl_2 solution at room temperature shows no sign of electrochemical activity between −1.6 and +1.6 V. When compound **1** in CH_2Cl_2 solution at 0 °C (ice bath) is exposed to a CO atmosphere, no CO uptake is observed to occur (IR spectroscopy), at least during 7 h. Unaltered starting material can be recovered from these solutions.

The structure of the anion $[Cr(C_6F_5)_5]^{2-}$ as established by X-ray diffraction analysis on single crystals of $\mathbf{1}\cdot CH_2Cl_2$ is depicted in Figure 1. A selection of bond lengths and angles is given in Table 2. The low value of the angular parameter $\tau = 0.14$[19] denotes an approximately square pyramidal (*SPY*-5) geometry with the apical position occupied by the C(25)−C(30) aryl ring. The Cr atom is located 31 pm above the best basal plane defined by the remaining C-donor atoms (with deviations of ca. ±8 pm). All the *ipso*-C atoms are strictly planar. Two *trans*-standing C_6F_5 groups are slightly staggered (mutual dihedral angle: 14.5°) and almost perpendicular to the basal plane (ca. 83°). They are not symmetrically bound to Cr with two noticeably different $Cr-C^{ipso}-C^{ortho}$ angles for each ring: 115.2(2)° versus 132.6(2)° and 109.3(2)° versus 138.6(2)°. This swing makes two *o*-F atoms approach the Cr center at distances that are

(15) Maslowsky, E., Jr. *Vibrational Spectra of Organometallic Compounds*; John Wiley & Sons: New York, 1977; pp 437−442. Usón, R.; Forniés, J. *Adv. Organomet. Chem.* **1988**, *28*, 219.

(16) *SAINT*, version 6.02; Bruker Analytical X-ray Systems: Madison, WI, 1999.

(17) Sheldrick, G. M. *SADABS empirical absorption program*, version 2.03; University of Göttingen: Göttingen, Germany, 1996.

(18) Sheldrick, G. M. *SHELXL-97*, *Program for the refinement of crystal structures from diffraction data*; University of Göttingen: Göttingen, Germany, 1997.

(19) For the definition and use of this geometric descriptor of five-coordinate molecules see: Addison, A. W.; Rao, T. N.; Reedijk, J.; van Rijn, J.; Verschoor, G. C. *J. Chem. Soc., Dalton Trans.* **1984**, 1349. Alvarez, S.; Llunell, M. *J. Chem. Soc., Dalton Trans.* **2000**, 3288.

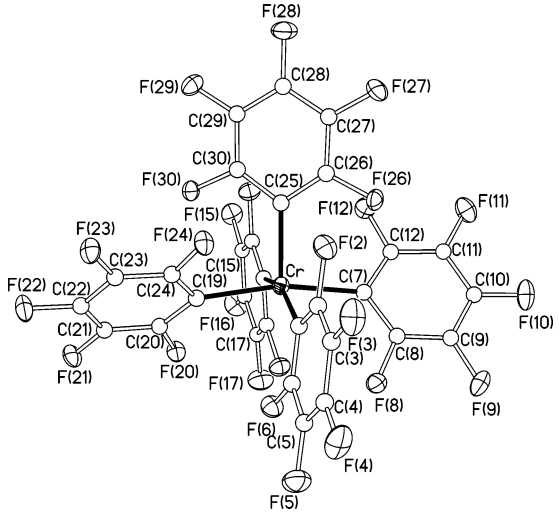

Figure 1. Thermal ellipsoid diagram (50% probability) of the anion of $[NBu_4]_2[Cr(C_6F_5)_5]$ (**1**).

Table 2. Selected Interatomic Distances and Angles and Their Estimated Standard Deviations for $1\cdot CH_2Cl_2$

Bond Distances (pm)			
Cr−C(1)	215.5(2)	C(13)−C(14)	137.6(3)
Cr−C(7)	218.5(2)	C(13)−C(18)	137.3(3)
Cr−C(13)	214.0(2)	C(14)−F(14)	136.8(2)
Cr−C(19)	216.5(2)	C(18)−F(18)	138.0(2)
Cr−C(25)	208.8(2)	C(19)−C(20)	138.6(3)
C(1)−C(2)	137.8(3)	C(19)−C(24)	138.5(3)
C(1)−C(6)	137.7(3)	C(20)−F(20)	136.5(2)
C(2)−F(2)	136.2(3)	C(24)−F(24)	136.8(2)
C(6)−F(6)	137.2(2)	C(25)−C(26)	138.7(3)
C(7)−C(8)	138.8(3)	C(25)−C(30)	138.3(3)
C(7)−C(12)	138.3(3)	C(26)−F(26)	137.0(2)
C(8)−F(8)	136.4(2)	C(30)−F(30)	136.5(2)
C(12)−F(12)	136.5(2)		
Bond Angles (deg)			
C(1)−Cr−C(7)	91.31(8)	C(7)−C(8)−F(8)	120.1(2)
C(1)−Cr−C(13)	159.06(9)	C(7)−C(12)−F(12)	120.5(2)
C(1)−Cr−C(19)	83.83(8)	Cr−C(13)−C(14)	138.64(18)
C(1)−Cr−C(25)	103.57(9)	Cr−C(13)−C(18)	109.26(17)
C(7)−Cr−C(13)	86.39(8)	C(14)−C(13)−C(18)	112.1(2)
C(7)−Cr−C(19)	167.57(9)	C(13)−C(14)−F(14)	120.7(2)
C(7)−Cr−C(25)	97.75(9)	C(13)−C(18)−F(18)	117.3(2)
C(13)−Cr−C(19)	94.06(8)	Cr−C(19)−C(20)	126.33(17)
C(13)−Cr−C(25)	97.36(9)	Cr−C(19)−C(24)	121.62(16)
C(19)−Cr−C(25)	94.52(9)	C(20)−C(19)−C(24)	112.0(2)
Cr−C(1)−C(2)	132.61(18)	C(19)−C(20)−F(20)	120.4(2)
Cr−C(1)−C(6)	115.20(17)	C(19)−C(24)−F(24)	120.4(2)
C(2)−C(1)−C(6)	112.2(2)	Cr−C(25)−C(26)	124.51(17)
C(1)−C(2)−F(2)	120.6(2)	Cr−C(25)−C(30)	123.59(17)
C(1)−C(6)−F(6)	118.7(2)	C(26)−C(25)−C(30)	111.8(2)
Cr−C(7)−C(8)	124.42(18)	C(25)−C(26)−F(26)	120.5(2)
Cr−C(7)−C(12)	123.92(17)	C(25)−C(30)−F(30)	120.5(2)
C(8)−C(7)−C(12)	111.4(2)		

still too long to be considered as indicative of any bonding interaction ($Cr\cdots F^{ortho} > 280$ pm), but probably exerting some protective effect toward the "vacant coordination site". The other two *trans*-standing C_6F_5 groups are almost completely staggered (mutual dihedral angle: 78°), more symmetrically coordinated to Cr, and considerably more tilted toward the basal plane (dihedral angles: ca. 50°). This tilting can be viewed as a way of minimizing repulsive effects with the *o*-F atoms of the apical C_6F_5 group. The latter is symmetrically coordinated to Cr with virtually identical $Cr-C^{ipso}-C^{ortho}$ angles; it is also rotated away from the C(7)−C(19) basal line by ca. 35°. Considering that the trigonal bipyramidal (*TBPY*-5) geometry is more suited to minimizing interligand repulsions, the fact that $[Cr(C_6F_5)_5]^{2-}$ in **1** adopts a *SPY*-5 structure must be due to electronic reasons associated with the metal center electron configuration (see below). However, the $C_{api}-Cr-C_{bas}$ angles [$\varphi_{av} = 98.3(1)°$] are surprisingly close to the theoretical value ($\varphi = 104°04'$) calculated for a *SPY*-5 geometry (C_{4v} symmetry) on the basis of a simple, purely electrostatic model.[20] The $Cr-C_{api}$ bond length [208.8(2) pm] is significantly shorter than the average $Cr-C_{bas}$ distance [216.1(2) pm]. This is in keeping with extended Hückel calculations on ML_5 species that predict stronger apical bonds for *SPY*-5 complexes with d^0-d^6 electron configuration.[21] It is worthwhile noting that the structure of the nonfluorinated anion $[CrPh_5]^{2-}$ in $[\{Na(OR_2)_2\}_2\{CrPh_5\}]$ has been described as a distorted *TBPY*-5.[9b] Although some influence of the different steric requirements and donor abilities[22] of the C_6X_5 groups (X = H or F) in the molecular geometries of the anions $[Cr(C_6X_5)_5]^{2-}$ cannot be ruled out, it is reasonable to assign their structural differences to the sharply different degree of ion association observed for both compounds in the solid state. Thus, while separate ions are found in the lattice of **1**, strong cation/anion interactions were observed in the nonfluorinated homologue in which the C_6H_5 rings are, in fact, bridging the Cr^{3+} and Na^+ centers. The importance of the nature of the cation/anion interaction in governing the molecular geometry and even the stoichiometry of a chemical species has been already demonstrated in organochromium chemistry. Thus, replacement of the THF molecules in $[Li(THF)]_4[Cr_2Me_8]$ by tmen causes the reversible cleavage of the Cr−Cr quadruple bond and formation of the monomeric, high-spin species $[Li(tmen)]_2[CrMe_4]$, both compounds showing strong cation/anion association.[23] It is also known that, in contrast to the stability of $Li_3CrPh_6\cdot nEt_2O$,[10a] the corresponding sodium salt undergoes spontaneous dissociation of 1 equiv of NaPh, giving $Na_2CrPh_5\cdot nEt_2O$.[9a] The existence of such strong cation/anion interactions is expected to have an especially important influence on the equilibrium geometry of a five-coordinate species, since the energy difference between the two most common polyhedra, *TPBY*-5 and *SPY*-5, is not, in general, very large.

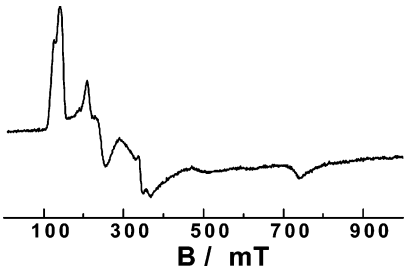

Figure 2. X-band EPR spectrum measured on a powder sample of **1** at 77.3 K.

EPR Measurements and Analysis. The X-band EPR spectrum of a powder sample of **1** measured at 77.3 K is shown in Figure 2. No significant modification is

(20) Zemann, J. *Z. Anorg. Allg. Chem.* **1963**, *324*, 241. φ has sometimes been referred to as the pyramidality angle.
(21) Rossi, A. R.; Hoffmann, R. *Inorg. Chem.* **1975**, *14*, 365.
(22) Tolman, C. A. *J. Am. Chem. Soc.* **1970**, *92*, 2953. Sheppard, W. A. *J. Am. Chem. Soc.* **1970**, *92*, 5419.
(23) Hao, S.; Gambarotta, S.; Bensimon, C. *J. Am. Chem. Soc.* **1992**, *114*, 3556.

observed by changing the measurement temperature from 77.3 K to room temperature. In every case, the magnetic field was swept up to 1.5 T, but no signals were observed above 1.0 T. The EPR spectroscopic behavior of **1** is in sharp contrast to that previously described for the pseudo-octahedral, homoleptic pentachlorophenyl species $[Cr^{III}(C_6Cl_5)_4]^-$.[8] The latter behaves as an apparent $S' = 1/2$ system, deriving from an $S = 3/2$ entity with a dominant zero-field contribution. The low magnetic-field resonances (at ca. 130 mT) in the EPR spectrum of **1** strongly suggest that the zero-field contribution in the five-coordinate pentafluorophenyl species $[Cr^{III}(C_6F_5)_5]^{2-}$ is comparable in magnitude with the operating microwave frequency (ca. 9−10 GHz in X-band). The EPR spectrum of **1** bears remarkable similarities with those reported for six-coordinate Werner-type Cr^{III} compounds such as $[Cr^{III}Cl_5(OH_2)]^{2-}$,[24] *trans*-$[Cr^{III}(ox)_4XX']^{n-}$,[25] *trans*-$[Cr^{III}(NH_3)_4XX']^{n+}$,[26,27] *trans*-$[Cr^{III}(py)_4XX']^{n+}$,[27] *trans*-$[Cr^{III}(en)_2X_2]^{n+}$,[28] or *trans*-$[Cr^{III}(cyclam)X_2]^{n+}$,[29] in which the Cr^{III} center is located in different tetragonal environments (ox = oxalato; cyclam = 1,4,8,11-tetraazacyclotetradecane; X, X′ = neutral or singly charged monodentate ligands). In all these cases an isotropic Zeeman contribution was assumed and the spin Hamiltonian used is given, in the principal axes of the zero-field contribution, by

$$H = g\mu_B \vec{\mathbf{B}}\cdot\vec{\mathbf{S}} + D\left[S_z^2 - \frac{1}{3}S(S+1)\right] + E(S_x^2 - S_y^2) \quad (2)$$

with $S = 3/2$ and where g represents the gyromagnetic factor, μ_B is the Bohr magneton, and D and E describe the zero-field contribution in the standard form.

On the basis of our experience in analyzing EPR spectra of $S = 1$ systems,[30] we have developed an ad hoc program for simulating EPR spectra of powder samples containing $S = 3/2$ entities, with the (possibly) orthorhombic $\tilde{\mathbf{g}}$-tensor being coaxial with the zero-field contribution. This approach has been found to be appropriate for a C_{2v} metal coordination environment. In addition to the X-band spectrum (Figure 2), room-temperature Q- and W-band spectra of **1** were also measured, the latter being shown in Figure 3. These spectra confirm the validity of our assignments.

Using the referred simulation program, different values of the zero-field contribution relative to the microwave frequency were screened and, as anticipated above, the best fitting with the real spectra was attained when the zero-field splitting between the two Kramers doublets was set near 10 GHz. In this case, the analysis of the higher-frequency W-band (operating at ν ca. 95 GHz) spectrum is considerably simpler, and hence we will focus on it. The central part (2.5−4.2 T) can be described, at least qualitatively, in the high magnetic-field limit. The energy levels are labeled in the standard way. Furthermore, the line appearing at ca. 1 T is assigned to the $|-3/2\rangle \leftrightarrow |+3/2\rangle$ transitions and confirms that we are dealing with an actual $S = 3/2$ system. The lines marked with a star in Figure 3 are assigned to the $|\pm 3/2\rangle \leftrightarrow |\pm 1/2\rangle$ transitions for an orientation of the magnetic field along one of the principal axes of the zero-field contribution. Following these assignments, an estimate of the spin-Hamiltonian parameter in terms of eq 2 can be carried out, and the results are given in Table 3. This assignment, however, cannot account for the features marked with a cross on the spectrum. We suggest that the crossed and the starred features in Figure 3 are due to two different Cr^{III} entities in the sample with very similar coordination environments, hereafter labeled center A and center B, respectively. In this context, it is worthwhile noting that EPR spectroscopy is a very sensitive tool, especially for $S > 1/2$ systems, providing in some instances information on local distortions that are imperceptible to other structural techniques including X-ray diffraction methods. Lattice effects are known to affect variations of the zero-field splitting tensor in the aforementioned $[Cr^{III}(NH_3)_5X]^{2+}$ complexes, while they exert little effect on the $\tilde{\mathbf{g}}$-tensor.[26b] The central features of the W-band EPR spectrum of **1** (see inset in Figure 3), corresponding to the $|+1/2\rangle \leftrightarrow |-1/2\rangle$ transitions along the principal axis, further suggest the existence of two Cr^{III} entities. The spin-Hamiltonian parameter for the second Cr^{III} center (center B) have also been estimated and are given in Table 3. These two sets of parameters allow us to account for all the features appearing in the X-, Q-, and W-band spectra of **1**. Although good agreement was achieved in the number of spectral features and their positions, the relative line-widths could not be exactly reproduced using Lorentzian line-shapes with isotropic line-widths. The need for anisotropic and transition-dependent line-width parameters when simulating spec-

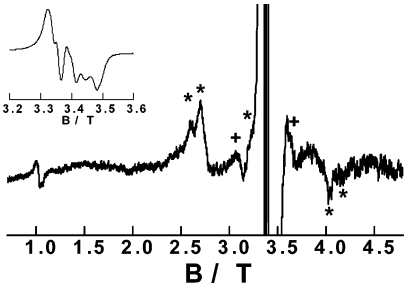

Figure 3. W-band EPR spectrum measured on a powder sample of **1** at room temperature. The inset shows a scaled and detailed view of the central part of the spectrum.

Table 3. Relevant Spin-Hamiltonian Parameters Derived from EPR Spectroscopic Data of 1

	center A[a]	center B[b]
g_x	2.00(1)	1.98(1)
g_y	1.99(1)	1.99(1)
g_z	1.98(1)	2.00(1)
D (GHz)	10.91(5)	13.2(1)
E/D	0.23(1)	0.14(2)

[a] Connected with the starred features in Figure 3. [b] Connected with the crossed features in Figure 3.

(24) (a) Mohrmann, L. E., Jr.; Garrett, B. B.; Lewis, W. B. *J. Chem. Phys.* **1970**, *52*, 535. (b) Garrett, B. B.; DeArmond, K.; Gutowsky, H. S. *J. Chem. Phys.* **1966**, *44*, 3393.
(25) Andriessen, W. T. M. *Inorg. Chem.* **1975**, *14*, 792.
(26) (a) Andriessen, W. T. M.; Meuldijk, J. *Inorg. Chem.* **1976**, *15*, 2044. (b) Holbrook, M. T.; Garrett, B. B. *Inorg. Chem.* **1976**, *15*, 150. (c) Pedersen, E.; Kallesoe, S. *Inorg. Chem.* **1975**, *14*, 85. (d) Baker, S. J.; Garrett, B. B. *Inorg. Chem.* **1974**, *13*, 2683. (e) Mohrmann, L. E., Jr.; Garrett, B. B. *Inorg. Chem.* **1974**, *13*, 357. See also ref 24a.
(27) Pedersen, E.; Toftlund, H. *Inorg. Chem.* **1974**, *13*, 1603.
(28) Hempel, J. C.; Morgan, L. O.; Lewis, W. B. *Inorg. Chem.* **1970**, *9*, 2064. McGarvey, B. R. *J. Chem. Phys.* **1964**, *41*, 3743.
(29) Solano-Peralta, A.; Sosa-Torres, M. E.; Flores-Alamo, M.; El-Mkami, H.; Smith, G. M.; Toscano, R. A.; Nakamura, T. *Dalton Trans.* **2004**, 2444. Ueki, S.; Yamauchi, J. *Inorg. Chim. Acta* **2002**, *338*, 13.
(30) Alonso, P. J.; Forniés, J.; García-Monforte, M. A.; Martín, A.; Menjón, B. *Chem. Commun.* **2001**, 2138.

tra of randomly oriented samples of Cr^{III} complexes had been already pointed out.[31]

The model for the electronic states of the anionic species $[Cr^{III}(C_6F_5)_5]^{2-}$ can be derived starting with a hypothetical octahedral "$[Cr^{III}(C_6F_5)_6]^{3-}$" anion from which one of the ligands has been removed. As a result of this *Gedankenexperiment*, the originally $^4A_{2g}$ ground state for the t_{2g}^3 electron configuration in an O_h symmetry would correlate to the also orbitally nondegenerate $^4B_1$ state corresponding to the $b_2(xy)^1\ e(xz,yz)^2$ electron configuration in an ideal *SPY*-5 (C_{4v}) environment. The real symmetry of the $[Cr^{III}(C_6F_5)_5]^{2-}$ anion as found in the crystal structure of **1**·CH_2Cl_2 is even lower (approximately C_2). This symmetry lowering would be expected to effect a splitting in the excited terms with two important consequences: (1) enabling some degree of admixture with the ground term, and (2) introducing the zero-field contribution. In any case, the *g* factors have been found to be close to 1.99 and almost isotropic, as is usually found for Cr^{III} paramagnetic entities.

Homoleptic Perhalophenyl Derivatives of Ti^{III} and Cr^{III}. While referring to transition-metal molecular species, it has been said that "it is difficult to determine what part of an observed conformation preference is due to electronic effects [...] and what part is set by the often large steric requirements of the coordinated ligands".[21] Admitting this inherent difficulty, the fact that homoleptic pentafluoro- and pentachlorophenyl derivatives are currently known for Ti^{III} (d^1) and Cr^{III} (d^3) is especially advantageous, since it allows us to establish useful comparisons between them.

Concerning the stoichiometry, five-substituted $[MR_5]^{2-}$ species are obtained with the C_6F_5 group (R) for the two metals [M = Ti,[32] Cr (**1**)], while with the more sterically demanding C_6Cl_5 group (R′), four-substituted $[MR'_4]^-$ anions are formed instead.[8,33] The different stoichiometry attained in each case can be reasonably attributed to purely steric reasons. On the other hand, the fact that all four species within the series considered here have different molecular geometries can be explained mainly in terms of the different electron configuration of each metal center.

C_6X_5 groups (X = F, Cl) have been assigned a marked electron-withdrawing character.[22] When σ-bound to electron-rich late transition metals, they are known to be able to act as π-acceptors of the excess of electron density on the metal, thereby conferring some multiple character to the M−C_6X_5 bond.[34] This model, however, would not be expected to apply to electron-poor transition metals, and thus, highly polar M^{III}−C_6X_5 bonds with a mainly σ-donor character can be anticipated for M = Ti, Cr. Highly polar M−L bonds and bulky ligands L both favor molecular structures close to those predicted in terms of interligand repulsion minimization in the absence of deciding electronic factors (ligand-close packing, LCP, model).[35] A d^1 electron configuration is usually considered to be stereochemically nonactive. According to this reasoning, a nearly tetrahedral (*T*-4) geometry has been found for the anion $[Ti(C_6Cl_5)_4]^-$,[33] while the five-substituted species $[Ti(C_6F_5)_5]^{2-}$ shows a roughly *TBPY*-5 structure.[32] The slight deviations from the ideal *T*-4 geometry in the former case ($T_d \rightarrow D_{2d}$ symmetry) have been attributed[12] to the highly anisotropic character of the C_6Cl_5 group, as suggested for a wide range of ER_4 molecules where R is a polyatomic monodentate substituent.[36] Since, in the case of the anion $[Ti(C_6F_5)_5]^{2-}$, an idealized *TBPY*-5 structure would lead to the orbitally degenerate state $e''(xz,yz)^1$, the experimentally observed symmetry lowering from D_{3h} to C_{2v} (Figure 4) has been attributed to the Jahn−Teller effect in combination with steric difficulties possibly encountered in arranging five C_6F_5 groups around a first-row transition-metal ion.[32]

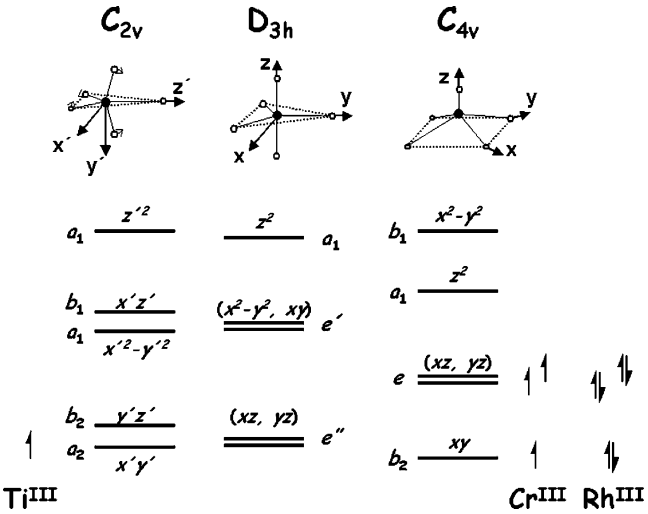

Figure 4. Relative d-orbital energy levels according to the idealized metal coordination environments for the homoleptic anions $[M(C_6F_5)_5]^{2-}$.

Since exactly the same steric requirements are associated with the Ti and Cr species within each isoleptic pair, any structural difference arising between them must be necessarily due to electronic reasons. Thus, in contrast to the results obtained for Ti^{III}, the anion $[Cr(C_6Cl_5)_4]^-$ has been found to exhibit a pseudo-octahedral structure since two of the C_6Cl_5 groups act as standard σ-bonded monodentate ligands (C_6Cl_5-κC), while the other two act as small-bite didentate ligands coordinated through both the *ipso*-C and one of the *ortho*-Cl atoms (C_6Cl_5-κC,κCl^2).[8] The marked preference of Cr^{III} to adopt an *OC*-6 geometry is well known[37] and can be related to the tendency to achieve half-occupation of the (*xy*,*xz*,*yz*) set giving a t_{2g}^3 level or configurations derived thereof by symmetry lowering. Well-established five-coordinate Cr^{III} compounds are, in turn, still rare.[38] The adoption by the $[Cr(C_6F_5)_5]^{2-}$ anion of a *TBPY*-5 geometry would lead to the orbitally degenerate electronic state $e''(xz,yz)^2\ e'(x^2-y^2,xy)^1$, which following the

(31) Bonomo, R. P.; di Bilio, A. J.; Riggi, F. *Chem. Phys.* **1991**, *151*, 323.
(32) Alonso, P. J.; Falvello, L. R.; Forniés, J.; García-Monforte, M. A.; Menjón, B. *Angew. Chem., Int. Ed.* **2004**, *43*, 5225.
(33) Alonso, P. J.; Forniés, J.; García-Monforte, M. A.; Martín, A.; Menjón, B. *Chem. Commun.* **2002**, 728. See also ref 12.
(34) Parshall, G. W. *J. Am. Chem. Soc.* **1966**, *88*, 704. Coulson, D. R. *J. Am. Chem. Soc.* **1976**, *98*, 3111.
(35) Gillespie, R. J.; Popelier, P. L. A., *Chemical Bonding and Molecular Geometry*; Oxford University Press: New York, 2001.
(36) Heard, G. L.; Gillespie, R. J.; Rankin, D. W. H. *J. Mol. Struct.* **2000**, *520*, 237.
(37) Cotton, F. A.; Wilkinson, G.; Murillo, C. A.; Bochman, M. *Advanced Inorganic Chemistry*, 6th ed.; John Wiley & Sons: New York, 1999; Section 17-C, pp 736−756.

Jahn−Teller theorem[39] should be unstable. Instead of introducing some distortion to split the orbital degeneracy, as observed in the Ti^{III} isoleptic species, the adoption of a *SPY*-5 geometry is preferred in this case. Attending to the d-orbital energy levels for *SPY*-5 geometry (C_{4v} symmetry in Figure 4),[21,40] the structural features observed for $[Cr(C_6F_5)_5]^{2-}$ and the EPR data available both suggest a $b_2(xy)^1\ e(xz,yz)^2$ configuration. Similar structural features would be expected for low-spin d^6 systems with $b_2(xy)^2\ e(xz,yz)^4$ configuration. Previous work failed to confirm this point by comparing five-coordinate Cr^{III} and Ir^{III} compounds containing tridentate ligands.[38c] It can be seen that the structure of d^3 $[Cr(C_6F_5)_5]^{2-}$ is indeed very similar to that of d^6 $[Rh(C_6F_5)_5]^{2-}$,[41] an observation that reinforces the validity of the model.

Concluding Remarks

The synthesis of the homoleptic σ-organochromium(III) compound $[NBu_4]_2[Cr(C_6F_5)_5]$ has allowed us to obtain structural information on simple $[CrR_5]^{2-}$ species free from the influence of strong cation/anion interactions. We believe this to be the first structurally characterized square pyramidal ML_5 species with d^3 configuration, where M is any transition metal and L any monodentate ligand.

A comparison of the metal coordination geometries of the isoleptic pairs $[M(C_6Cl_5)_4]^-$ and $[M(C_6F_5)_5]^{2-}$ (M = Ti or Cr) allows us to assign to what extent the experimentally observed structures in each case are due to electronic or steric effects. It is concluded that in the case of Ti^{III} with a d^1 stereochemically nonactive electron configuration steric reasons are dominating, and thus, the observed structures of $[Ti(C_6Cl_5)_4]^-$ and $[Ti(C_6F_5)_5]^{2-}$ are near those expected following the ligand close-packing (LCP) model. In the case of Cr^{III}, in turn, the pseudo-octahedral and *SPY*-5 structures found for $[Cr(C_6Cl_5)_4]^-$ and $[Cr(C_6F_5)_5]^{2-}$, respectively, seem to be mainly due to electronic reasons associated with the d^3 electron configuration of the metal center.

Acknowledgment. This work has been supported by the Spanish MCYT (DGI)/FEDER (Project BQU2002-03997-CO2-02) and the Gobierno de Aragón (Grupo Consolidado: Química Inorgánica y de los Compuestos Organometálicos). The Gobierno de Aragón is also acknowledged for a grant to M.A.G.-M. We are indebted to Dr. Inés García Rubio (EPR Research Group at the ETH Zürich, Switzerland) for kindly providing the W-band EPR data.

Supporting Information Available: Crystallographic data of $[NBu_4]_2[Cr(C_6F_5)_5]\cdot CH_2Cl_2$ (CIF format). This material is available free of charge via the Internet at http://pubs.acs.org.

OM0499106

(38) (a) MacAdams, L. A.; Kim, W. K.; Liable-Sands, L. M.; Guzei, I. A.; Rheingold, A. L.; Theopold, K. H. *Organometallics* **2002**, *21*, 952. (b) Gibson, V. C.; Newton, C.; Redshaw, C.; Solan, G. A.; White, A. J. P.; Williams, D. J. *J. Chem. Soc., Dalton Trans.* **2002**, 4017. (c) Gibson, V. C.; Mastroianni, S.; Newton, C.; Redshaw, C.; Solan, G. A.; White, A. J. P.; Williams, D. J. *J. Chem. Soc., Dalton Trans.* **2000**, 1969. (d) Fryzuk, M. D.; Leznoff, D. B.; Rettig, S. J.; Young, V. G. *J. Chem. Soc., Dalton Trans.* **1999**, 147. (e) Gibson, V. C.; Maddox, P. J.; Newton, C.; Redshaw, C.; Solan, G. A.; White, A. J. P.; Williams, D. J. *Chem. Commun.* **1998**, 1651. (f) Fryzuk, M. D.; Leznoff, D. B.; Rettig, S. J. *Organometallics* **1997**, *16*, 5116. (g) Cotton, F. A.; Czuchajowska, J.; Falvello, L. R.; Feng, X. *Inorg. Chim. Acta* **1990**, *172*, 135. (h) Greene, P. T.; Russ, B. J.; Wood, J. S. *J. Chem. Soc. A* **1971**, 3636. See also ref 9.

(39) Jahn, H. A.; Teller, E. *Proc. R. Soc. (London) A* **1937**, *161*, 220.

(40) Holmes, R. R. *J. Am. Chem. Soc.* **1984**, *106*, 3745. Wood, J. S. *Prog. Inorg. Chem.* **1972**, *16*, 227. Furlani, C. *Coord. Chem. Rev.* **1968**, *3*, 141.

(41) García, M. P.; Oro, L. A.; Lahoz, F. J. *Angew. Chem., Int. Ed. Engl.* **1988**, *27*, 1700.